JOM
https://doi.org/10.1007/s11837-017-2731-x

Additive Manufacturing of Syntactic Foams: Part 2: Specimen Printing and Mechanical Property Characterization

ASHISH KUMAR SINGH,[1] BROOKS SALTONSTALL,[1] BALU PATIL,[2] NIKLAS HOFFMANN,[3] MRITYUNJAY DODDAMANI,[2] and NIKHIL GUPTA[1,4]

1.—Composite Materials and Mechanics Laboratory, Mechanical and Aerospace Engineering Department, New York University, Tandon School of Engineering, Brooklyn, NY 11201, USA. 2.—Advanced Manufacturing Laboratory, Department of Mechanical Engineering, National Institute of Technology Karnataka, Surathkal, India. 3.—Institut für Maschinenwesen, Technische Universität Clausthal, Clausthal, Zellerfeld, Germany. 4.—e-mail: ngupta@nyu.edu

High-density polyethylene (HDPE) and its fly ash cenosphere-filled syntactic foam filaments have been recently developed. These filaments are used for three-dimensional (3D) printing using a commercial printer. The developed syntactic foam filament (HDPE40) contains 40 wt.% cenospheres in the HDPE matrix. Printing parameters for HDPE and HDPE40 were optimized for use in widely available commercial printers, and specimens were three-dimensionally (3D) printed for tensile testing at strain rate of 10^{-3} s^{-1}. Process optimization resulted in smooth operation of the 3D printer without nozzle clogging or cenosphere fracture during the printing process. Characterization results revealed that the tensile modulus values of 3D-printed HDPE and HDPE40 specimens were higher than those of injection-molded specimens, while the tensile strength was comparable, but the fracture strain and density were lower.

INTRODUCTION

Fused filament fabrication (FFF) is among the most widely used additive manufacturing (AM) methods due to its relatively simple process and the availability of filaments of a wide range of materials. FFF uses thermoplastic filaments to deposit layers of material through a nozzle to build the part based on a computer-aided design file. There is significant interest in developing filaments of new polymers and high-performance composites so that parts made from these materials can be printed for industrial applications. Recent studies have been successful in developing filaments that are reinforced with carbon fibers and carbon nanotubes.[1]

One of the possibilities for structural weight reduction is to use filaments of lightweight materials for FFF. Hollow particle-filled composites, called syntactic foams, have been used in weight-sensitive marine and aerospace applications.[2,3] Thermoplastic syntactic foams were proposed in the late 1960s, but progress on these materials has been slow. New manufacturing capabilities for these materials can benefit marine and automotive applications.[4,5] The present work is focused on developing high-density polyethylene (HDPE) matrix syntactic foam filament reinforced with fly ash cenospheres for use in FFF. The printing parameters were optimized to enable high-quality printing using a commercial FFF 3D printer. The same material system has previously been processed through injection and compression molding techniques.[6,7] Tensile test results obtained from the 3D-printed parts were compared with those from previous studies on injection and compression molding to determine the possibility of deploying such 3D-printed parts in suitable applications.

MATERIALS AND METHODS

Filament Material

Neat HDPE in the form of granules of HD50MA180 grade was procured from Reliance Polymers, Mumbai, India. Cenospheres (CIL-150) were procured from Cenosphere India Pvt. Ltd. for

Published online: 16 January 2018

Table I. Pilot study print settings

Parameter	Trial 1	Trial 2	Trial 3	Trial 4
Infill (%)	100	100	60	60
Layer thickness (mm)	0.27	0.35	0.35	0.35
Feed rate (mm/s)	35	35	30	30
Print head travel rate (mm/s)	35	35	30	30
Print temperature (°C)	250	250	250	250
Surface temperature (°C)	110	110	125	115
Air cooling	On	On	On	Off

use as filler. The first drawn HDPE40 filament had porosity due to incomplete penetration of resin between particles, therefore the filament was cut and redrawn (HDPE40-2X) and the drawing cycle repeated one more time (HDPE40-3X)0.[8] These two types of filaments were used in printing.

CAD Modeling and 3D Printing

ASTM D638 tensile specimens (types I and IV, see Supplementary Fig. S1) were modeled using SolidWorks© and converted to STL format with fine resolution setting. The STL models were then sliced to generate the tool path using ReplicatorG software. The specimen was oriented horizontally along the x-axis of the print bed. One shell and a 60% infill were chosen through optimization for the print, as explained in "3D Printing and Optimization" section

A Flashforge Creator Pro 3D printer was used in the study. To ensure adhesion of the bottom layer, an HDPE plate was used as the build platform. ASTM D638 type I tensile specimens were printed using HDPE, whereas type IV specimens were printed using HDPE40.

Imaging and Characterization

A Hitachi S-3200 N scanning electron microscope was used for microscopic observations. A Cressington 108 auto sputter coater was used for gold coating of the specimens before imaging.

An Instron 4467 universal testing machine was used to conduct tensile testing at initial strain rate of 10^{-3} s^{-1}. Instron digital extensometers with 1-inch and 2-inch gauge length were used to measure strain for type IV and type I specimens, respectively. Engineering stress and engineering strain values are reported in this work.

RESULTS AND DISCUSSION

3D Printing and Optimization

Pilot studies were conducted to determine the optimum settings for printing with the HDPE40 filament. Specimens with dimensions of $25 \times 12 \times 6$ mm^3 were printed using the parameters listed in Table I for each trial setting. Presence of ceramic particles in syntactic foams has been shown to reduce their coefficient of thermal expansion.[9] Such materials would show less shrinkage upon cooling, making them useful for developing 3D-printing methods to obtain parts with close dimensional tolerances. Several initial trials in the pilot study did not result in high-quality specimens.

Fig. 1. 3D-printed (a) HDPE and (b) HDPE40-2X tensile bar.

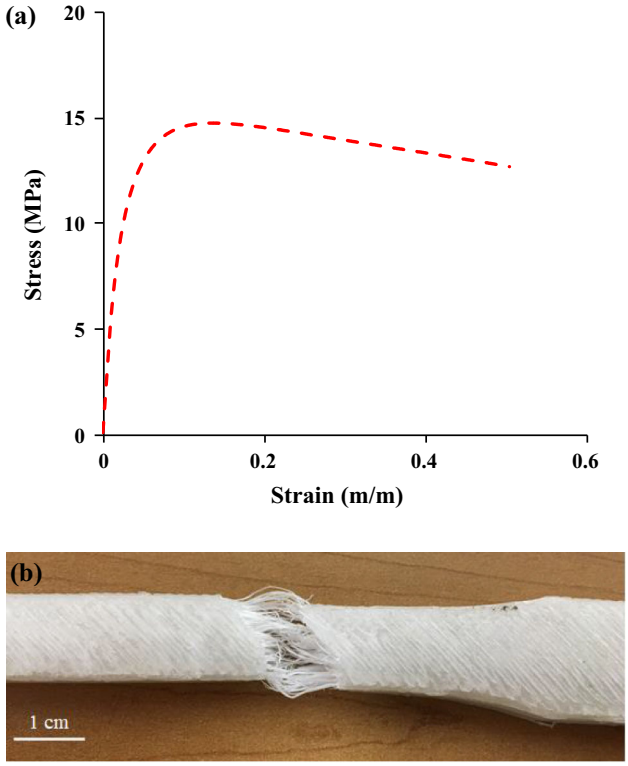

Fig. 2. (a) Representative stress–strain curve for HDPE tensile samples at strain rate of 10^{-3} s^{-1}, and (b) failure mode for HDPE tensile bar at 50% strain.

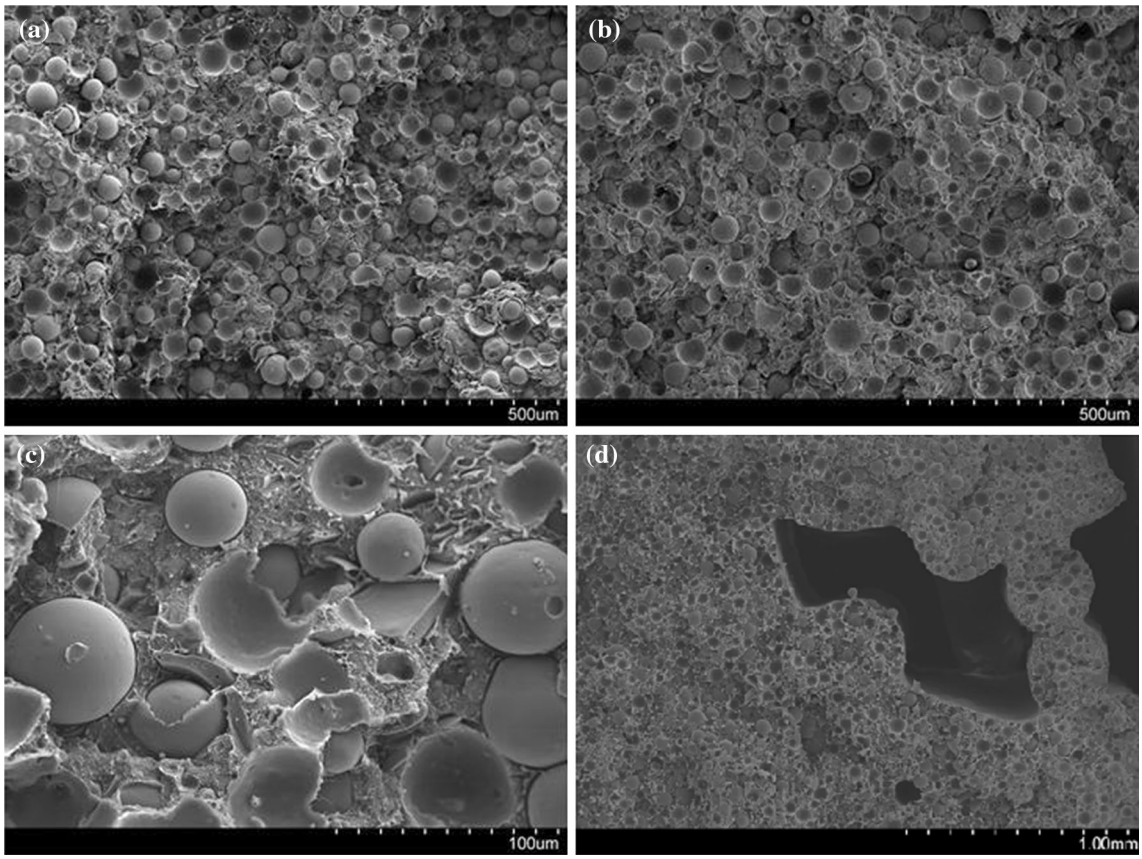

Fig. 3. Micrographs showing uniform distribution of cenospheres in 3D-printed (a) HDPE40-2X and (b) HDPE40-3X. (c) High-magnification micrograph of HDPE40-2X showing cenospheres that survived the filament manufacturing and 3D printing process. (d) A defect in HDPE40-2X specimen where incomplete filling is observed.

The most significant failure was the development of a bulge in the body of the printed part, which was the result of an excess volume of molten material constrained within the solidified shell which shrinks. The bulge grew as the printing continued and eventually started to interact with the print head. To minimize such bulging, the layer height was increased from 0.27 mm to 0.35 mm to allow higher clearance above the part. This change significantly reduced bulging. Subsequent trials resulted in reducing the feed rate and travel feed rate from 35 mm/s to 30 mm/s, which improved the surface finish, and reduced warpage in the specimens. Optimization of additional parameters such as increasing the print bed temperature from 110°C to 125°C reduced the warping effect at the face of the build that lies away from the cooling fan, but deformed the bottom of the part as more material is deposited on top. The infill percentage was lowered from 100% to 60% to further reduce the amount of extruded material within the solidified shell. These trials resulted in understanding of the effect of each parameter on the build quality.

Based on the initial tests, the build platform temperature was reduced from 125°C to 115°C to allow cooling of the bottom layer so that it can support the weight of layers above; the air cooling fan was disabled to allow slow and uniform cooling, and the printing surface was covered with a thin sheet of neat HDPE for better adhesion. The optimized print settings used for trial setting 4 (Table I) were then used to print the tensile test specimens. The infill pattern is at 45° to the x-axis (Supplementary Fig. S1). Examples of two 3D-printed HDPE and HDPE40-2X tensile specimens are shown in Fig. 1.

Density

The density of 3D-printed HDPE specimens is 0.855 ± 0.012 g/cm^3, which is 19% lower than for injection-molded HDPE (1.056 g/cm^3). Such a drop in density was also observed for the 3D-printed syntactic foams as well. The density of HDPE40-2X was 0.95 g/cm^3, which is 6% and 2% lower than injection-molded HDPE40 and HDPE40-2X filaments,[8] respectively. This decrease in density of the 3D-printed specimens is attributed to presence of porosity between layers.

Tensile Behavior

A representative stress–strain graph for a 3D-printed HDPE specimen is shown in Fig. 2a. Tests were stopped at 50% strain. The linear section in

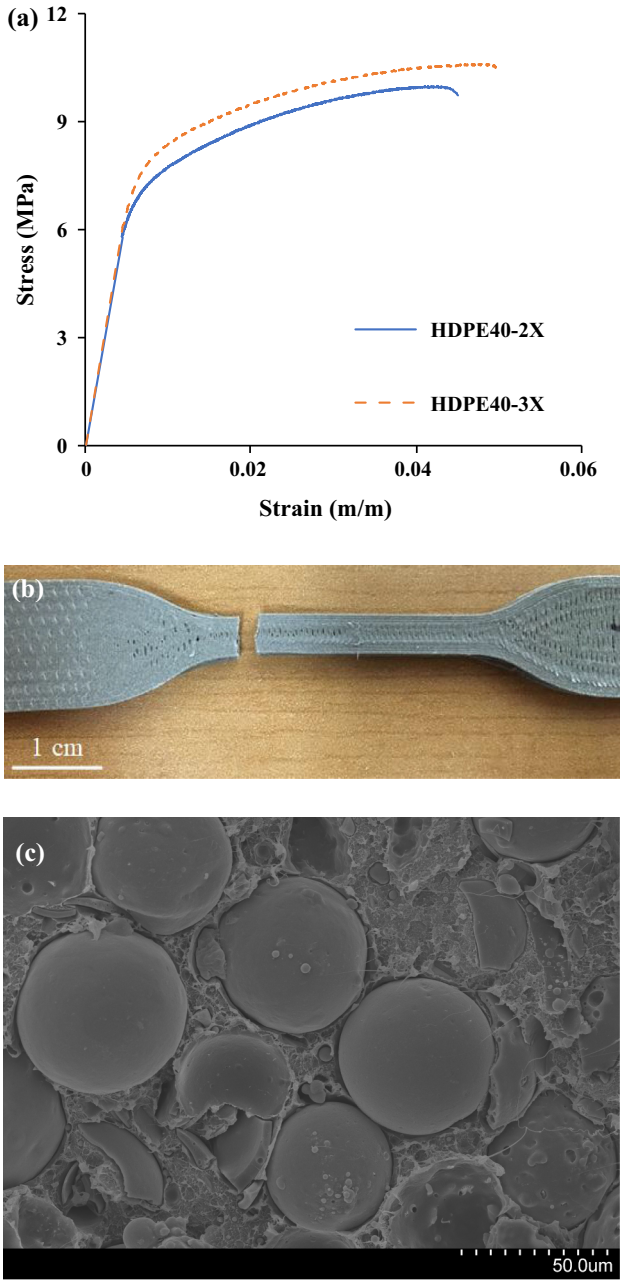

Fig. 4. (a) Representative stress–strain plots for 3D-printed HDPE40-2X and HDPE40-3X tensile specimens, (b) failure mode in HDPE40-2X specimen, and (c) intact cenospheres on fracture surface of tensile-tested HDPE40-3X specimen.

the elastic region was used to calculate the modulus, and the yield strength was obtained using the 0.2% offset method. The plot showed a peak at 13% strain, followed by a slow drop in stress. The elastic modulus, yield strength, and ultimate tensile strength were found to be 632 ± 76 MPa, 6.6 ± 0.6 MPa, and 14.3 ± 0.3 MPa, respectively. 3D-printed HDPE showed 18% higher modulus and 17.5% lower yield strength compared with the extruded filament at strain rate of 10^{-3} s^{-1}. Compared with injection-molded HDPE, the modulus of 3D-printed HDPE was 16% higher.[6] The failure mode of a 3D-printed HDPE specimen at 50% strain is shown in Fig. 2b, where a fibrous fracture is observed due to elongation of individual filaments extended in longitudinal directions, which causes separation of the printed layers. Although 3D-printed specimens performed comparably to molded specimens, further process improvements could be conducted to obtain monolithic specimens from 3D printing.

Imaging studies on HDPE40 specimens showed a uniform distribution of cenospheres throughout the cross-section of specimens printed with 2X (Fig. 3a) and 3X (Fig. 3b) filaments. Intact cenospheres are visible in the high-magnification micrograph (Fig. 3c), indicating high survival rate through two and three rounds of extrusion during filament manufacturing and the 3D printing process. Cenospheres with mean diameter of 76 ± 32 μm can be used with a printing nozzle diameter of 200 μm without any clogging.[10] Some of the specimens showed defects in the form of porosity in incompletely fused layers at certain locations (Fig. 3d). However, process optimization successfully reduced these defects and provided specimens with density close to the predicted value.

The tensile behavior of a representative set of 3D-printed HDPE40-2X and 3X specimens is compared in Fig. 4a. Unlike HDPE samples, the stress–strain curves do not show a peak, and the stress rises with strain until failure due to the increased brittleness of the material caused by the presence of ceramic particles. The failure strain was less than 6% for all the 3D-printed HDPE40 specimens, which is 30% to 40% lower than for HDPE40 filaments,[8] indicating that the material became brittle after the 3D printing process. The failure of HDPE40-2X was brittle in nature, as shown in Fig. 4b. The tensile modulus of 3D-printed HDPE40-2X and 3X (Table - II) was 1.6 and 2.6 times higher than that of 2X and 3X filaments, respectively.[8] This enhancement is likely due to additional crosslinking and realignment of polymer chains during the high-temperature extrusion process during printing, as suggested by some previous studies.[11,12] Crystallization of HDPE due to thermal gradients can also contribute to such enhancement in mechanical properties.[13] The fracture surface of a HDPE-2X specimen is shown in Fig. 4c. The primary failure mode of the specimens was matrix fracture by plastic deformation. Cenospheres were intact on the fracture surface.

The specific modulus of molded HDPE40 obtained in an earlier study at strain rate of 1.6×10^{-2} s^{-1} was 717 ± 27 MPa cm^3/g, which is 51% and 44% of that of 3D-printed HDPE-2X and 3X specimens tested at 10^{-3} s^{-1}.[6,14] The mechanical properties of HDPE–cenosphere syntactic foams are highly strain rate sensitive and show an increasing trend

Table II. Tensile properties of 3D-printed HDPE40-2X and 3X specimens

Material	Elastic modulus (MPa)	Density (g/cm^3)	Specific elastic modulus (MPa cm^3/g)	Yield strength (MPa)	Ultimate tensile strength (MPa)	Fracture strain (%)
HDPE40-2X	1337 ± 109	0.950	1407 ± 115	7.0 ± 0.4	10.1 ± 0.1	5.2 ± 0.5
HDPE40-3X	1569 ± 143	0.959	1636 ± 149	7.4 ± 0.5	10.7 ± 0.2	5.1 ± 0.1
Molded HDPE40[6]	723 ± 27	1.0078	717 ± 27	–	12.1 ± 0.44	9.42 ± 0.72

with strain rate.[8,10] Therefore, it is expected that the mechanical properties of 3D-printed HDPE40-2X and 3X will be even higher at comparable strain rates.

CONCLUSION

HDPE and HDPE40 filaments were used for 3D printing of tensile test specimens. Printing parameters for HDPE40 were optimized, and 3D-printed parts were subjected to tensile testing at strain rate of 10^{-3} s^{-1}. The tensile properties of 3D-printed specimens were compared with those of injection-molded specimens. The results can be summarized as follows:

- Warping of the specimen was reduced and quality was improved by optimizing the printer speed, layer thickness, print temperature, and cooling conditions.
- 3D-printed HDPE had 18% higher modulus and 17.5% lower yield strength than the HDPE filament.
- The microstructure of 3D-printed HDPE40 was similar to that of molded HDPE40. Cenospheres were uniformly distributed and survived the 3D printing process.
- The specific modulus of 3D-printed HDPE40-2X and 3X was 1.6 and 2.6 times higher than the respective filaments, but the fracture strain decreased by up to 40%.
- Comparison of specific mechanical properties showed promise for such 3D-printed syntactic foam components to replace some molded specimens for weight-reduction applications.

ACKNOWLEDGEMENTS

Mrityunjay Doddamani acknowledges Department of Science and Technology, India, Grant DST/TSG/AMT/2015/394/G and Visiting Scientist Fellowship Grant VSP 17-7-001 by the U.S. Office of Naval Research—Global (program manager Dr. Ramesh Kolar) to visit NYU for this work. Nikhil Gupta acknowledges Office of Naval Research Grant N00014-10-1-0988. The views expressed in this article are those of the authors, not of funding agencies.

ELECTRONIC SUPPLEMENTARY MATERIAL

The online version of this article (https://doi.org/10.1007/s11837-017-2731-x) contains supplementary material, which is available to authorized users.

REFERENCES

1. K. Kim, J. Park, J.-H. Suh, M. Kim, Y. Jeong, and I. Park, *Sens. Actuators A: Phys.* 263, 493–500 (2017).
2. N. Gupta, S.E. Zeltmann, V.C. Shunmugasamy, and D. Pinisetty, *JOM* 66, 245–254 (2014).
3. N. Gupta, D. Pinisetty, and V.C. Shunmugasamy, *Reinforced Polymer Matrix Syntactic Foams: Effect of Nano and Micro-Scale Reinforcement* (Berlin: Springer, 2013).
4. W.A. Waite, M.L. Waldron, and A. Nahabedian, *Naval Eng. J.* 81, 95–98 (1969).
5. H. Mae, M. Omiya, and K. Kishimoto, *Mater. Sci. Eng., A* 477, 168–178 (2008).
6. B.R. Bharath Kumar, M. Doddamani, S.E. Zeltmann, N. Gupta, M.R. Ramesh, and S. Ramakrishna, *Mater. Des.* 2016, 414–423 (2016).
7. M.L. Jayavardhan, B.R. Bharath Kumar, M. Doddamani, A.K. Singh, S.E. Zeltmann, and N. Gupta, *Compos. Part B: Eng.* 130, 119–131 (2017).
8. A.K. Singh, B. Patil, N. Hoffmann, B. Saltonstall, M. Doddamani, and N. Gupta, *JOM* (2018). https://doi.org/10.1007/s11837-017-2734-7.
9. V.C. Shunmugasamy, D. Pinisetty, and N. Gupta, *J. Mater. Sci.* 47, 5596–5604 (2012).
10. B.R. Bharath Kumar, A.K. Singh, M. Doddamani, D.D. Luong, and N. Gupta, *JOM* 68, 1861–1871 (2016).
11. J.J.C. Picot, *Polym. Eng. Sci.* 24, 415–420 (1984).
12. M. Yamaguchi and K.-I. Suzuki, *J. Appl. Polym. Sci.* 86, 79–83 (2002).
13. Y. Bin, D. Yan-Li, L. Gui-Jing, M. Ji-Bin, X. Ru, Q. Jia-Sheng, C. Peng, and L. Jing-Wang, *IOP Conf. Series: Mater. Sci. Eng.*, 87, (2015).
14. B.R.B. Kumar, M. Doddamani, S.E. Zeltmann, N. Gupta, and S. Ramakrishna, *Data Brief* 6, 933–941 (2016).